Ferrocene Functionalized Single-Walled Carbon Nanotube Bundles. Hybrid Interdigitated Construction Film for L-Glutamate Detection

Xing-Jiu Huang,*,† Hyung-Soon Im,† Do-Hoon Lee,‡ Hak-Sung Kim,‡ and Yang-Kyu Choi*,†

Nano-Bio-Electronic Lab, Department of Electrical Engineering and Computer Science and Department of Biological Sciences, Korea Advanced Institute of Science and Technology, 373-1 Guseong-dong, Yuseong-gu, Daejeon, South Korea

Received: September 4, 2006; In Final Form: November 9, 2006

A ferrocene functionalized SWCNT noncovalent nanohybrid was investigated by using a ferrocene/SWCNT interdigitated construction film as an electrode for L-glutamate detection. Ferrocene could immobilize on the surface of SWCNT bundles, and the ferrocene/SWCNT hybrid had a high stability not only in water but also in an organic solvent such as ethanol and acetone (no sediment was observed for more than 3 months). The nanohybrid could not only be thoroughly dispersed in ethanol but also adhere tightly onto glass substrates to form an interdigitated construction film. Owing to the existence of more carbon nanotubes, more active electrochemical mediators, and the unique interdigitated structure of the film, the ferrocene/SWCNT electrode exhibited a high catalytic efficiency, high sensitivity, and fast response during the detection of a low concentration of L-glutamate (1 μM). A good linear relationship between current and concentration was obtained from 1 to 7 μM.

1. Introduction

Carbon nanotubes are an attractive material for applications in electronic or sensor devices.[1,2] Numerous research on carbon nanotube functionalization (the edges or ends) with chemical groups that enable the binding of the carbon nanotube to other units or surfaces has been reported.[3,4] Especially, it has been found that many systems with aromatic rings and single-walled carbon nanotubes (SWCNT) via noncovalent bonding have been pursued in the past few years.[5] Ferrocene is well-studied as a mediator for electrochemical biosensing due to its good stability, high degree of characterization, and application potential for bioanalysis.[6] However, there are few reports on bioelectrochemical properties of ferrocene functionalized SWCNT. Recently, the functionalization of SWCNT with ferrocene in a covalent way and photoinduced electron transfer within the SWCNT−ferrocene nanohybrid were reported.[7] To our knowledge, although ferrocene derivatives were reported for biosening applications with carbon nanotubes,[8] only one study has been reported on the noncovalent assembly of a ferrocene/SWCNT hybrid system, but no bio-function or biosensor properties of the system were addressed.[9]

Aspartate aminotransferase (AST, EC 2.6.1.1) and alanine aminotransferase (ALT, EC 2.6.1.2) are enzymes found mainly in the liver but are also found in red blood cells, heart cells, muscle tissue, and other organs, such as the pancreas and kidneys. When body tissue or an organ such as the liver or heart is diseased or damaged, additional AST and ALT are released into the bloodstream, causing levels of the enzyme to rise, as the amount of AST and ALT in the blood is directly related to the extent of tissue damage.[10] Therefore, it is significant to determine AST and ALT amounts due to the clinical importance of AST and ALT in monitoring patients with liver diseases. AST and ALT are also biological catalysts, and the assay of all AST and ALT activity is based on the following enzyme reactions:

$$\text{L-aspartate} + \alpha\text{-ketoglutarate} \xrightarrow{\text{AST}} \text{oxalacetate} + \text{L-glutamate} \quad (1)$$

$$\text{L-alanine} + \alpha\text{-ketoglutarate} \xrightarrow{\text{ALT}} \text{pyruvate} + \text{L-glutamate} \quad (2)$$

As can be seen from eqs 1 and 2, L-glutamate was produced by AST and ALT, so L-glutamate is considered to be an important analyte to determine the activity of AST and ALT. A large number of papers have reported glutamate sensing materials including a chitosan enzyme film,[11] polymer/enzyme composite,[12] DNA-Cu(II)/polyamine membrane,[13] nanoparticle iridium/carbon film electrode,[14] and so on. In particular, Boo et al. reported a glutamate biosensor based on a nanoneedle consisting of a multiwalled carbon nanotube attached to the end of an etched tungsten tip.[15] Inspired by this case, here, we developed the investigation on ferrocene/SWCNT noncovalent nanohybrids in an alternative strategy by using a ferrocene functionalized SWCNT interdigitated construction film as an electrode for L-glutamate detection. We found that ferrocene could immobilize on the surface of SWCNT bundles and that the ferrocene/SWCNT hybrid had a high stability not only in water but also in an organic solvent such as ethanol and acetone. Furthermore, the nanohybrid could not only be thoroughly dispersed in ethanol but also adhere tightly onto glass substrates, like paint. Such an advantage enables us to obtain a uniform film that remains undamaged even after being dipped into an aqueous solution for a few months. The system reveals efficient biosensing functions.

* Corresponding author. Tel.: 82-42-869-8077. E-mail: (X.-J.H.) xingjiuhuang@hotmail.com and (Y.-K.C.) ykchoi@ee.kaist.ac.kr.
† Department of Electrical Engineering and Computer Science.
‡ Department of Biological Sciences.

10.1021/jp065747b CCC: $37.00
Published on Web 12/19/2006

2. Experimental Procedures

Materials. L-Glutamate acid monosodium salt monohydrate (EC No.: 2055381) and ferrocene (EC No.: 2030393) were purchased from Sigma-Aldrich. SWCNT (1−10 nm in diameter, 5−20 μm in length) was obtained from Iljin Nanotech Co., Ltd. Other reagents were commercially available and were of analytical grade. Double deionized water (DDW) was used in all measurements. A phosphate-buffered saline solution (PBS, pH 7.4) was prepared by dissolving 1.6 g of KCl, 64 g of NaCl, 1.92 g of KH_2PO_4, and 11.52 g of K_2HPO_4 in 800 mL of DDW. The L-glutamate solution was prepared in PBS, and the concentration was adjusted to be 0.01 M. The prepared solution was stored at 4 °C. The ferrocene solution was prepared by using ethanol, and the concentration was 0.01 M. Ag/AgCl (saturated KCl solution) electrodes were purchased from CH Instruments, Inc., and the Pt wire electrode was obtained from Bioelectrical System, Inc.

Synthesis of Ferrocene/SWCNT Bundle Hybrid Materials. First, 2 mg of raw SWCNT was chemically shortened by oxidation in a 10 mL mixture of concentrated sulfuric and nitric acids (3:1, 98 and 70%, respectively[16]), and this mixture was subjected to sonication for 8 h at 40 °C in the water bath. This procedure introduces carboxylic acid functionalities and defects at the ends of the nanotubes as well as some carboxylic acid units at the sidewalls.[2h,3a] The shortened SWCNT was then collected first by filtering using 0.1 μm nitrocellulose membranes (Advantec MFS, Inc.) and washed until a neutral pH was achieved. After dispersion in ethanol, the shortened SWCNT was found to be able to form a stable colloidal suspension. Second, ferrocene was immobilized onto the SWCNT surface by adding 500 μL of a 2 mg L^{-1} SWCNT solution to 50 mL of a 0.01 mM ferrocene solution and shaking at room temperature overnight. Thereafter, the mixture was centrifugally separated for removing the excessive ferrocene and finally re-dispersed in ethanol using sonication. This process was repeated several times.

Electrode Preparation. A glass slide (0.5 cm × 0.5 cm was cleaned by treatment with a freshly prepared mixture of 98% concentrated sulfuric acid and 30% H_2O_2 (volume ratio 7:3) at 95 °C for 30 min. An ethanol solution of ferrocene/SWCNT was then deposited to the glass slide and dried at room temperature, followed by exhaustive washing using ethanol and DDW and then dried again at ambient conditions. Similarly, this process was repeated several times. Typically, 50, 100, 150, and 200 μL of a ferrocene/SWCNT solution formed the needed composite film. The thickness of the final dried ferrocene/SWCNT film, which depends on the deposition cycle, can be determined by SEM experiments from a side view. Resistivities of the films were 39.33, 37.22, 29.90, and 26.97 Ω cm (coded as #1, #2, #3, and #4), respectively, as measured by a four point probe. In the experiment, the deposition cycle was defined as the process performed from dropping the first ferrocene/SWCNT solution to a second one. A working electrode was made by welding a platinum wire onto the ferrocene/SWCNT film with silver paste. After this, the electrode was partly mounted with epoxy resin, and a small area of film was left exposed, which was used to measure the electrochemical properties of the electrode, as well as to detect L-glutamate.

Characterization. Tapping mode AFM was done with a Nanoscope III (Digital Instruments, Veeco Metrology, LLC) scanning probe microscope. FTIR was performed using a model MB-154 analyzer (Bomem, Inc.). TEM images were obtained with a FEI Tecnai F20 transmission electron microscope. UV−vis was performed using a Cary 5E UV−vis/NIR spectrometer.

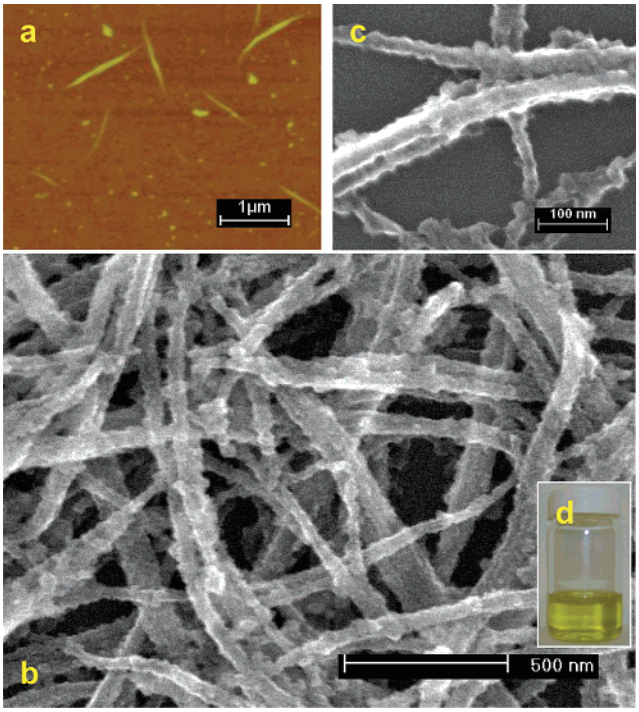

Figure 1. (a) Typical AFM image of dispersed shortened SWCNTs (after sonication for 8 h at 40 °C); some are aggregates of several tubes in van der Waals contact. (b) SEM image of ferrocene functionalized SWCNT bundles. (c) Enlarged SEM image. (d) Picture of well-dispersed ferrocene/SWCNT ethanol solution.

All of the SEM images were obtained with a Philips XL 30 AFEG scanning electron microscope). The Raman scattering measurements were carried out using an ISA Jobin-Yvon U-1000 spectrometer with a double monochromator and the 488 nm line of an argon laser.

Electrochemical Measurements. Cyclic voltammetry measurements were performed on a BAS 50W electrochemical analyzer (Bioanalytical Systems, Inc.). All CV experiments were carried out in PBS solution in a conventional three-electrode cell at room temperature. An Ag/AgCl and a Pt wire were employed as a reference and counter electrode, respectively. For amperometry, 200 mV was applied as an operating potential. After initial current decrease and stabilization, 1 μL of the L-glutamate solution was added at appropriate time intervals (300 s) to stabilize the signal between additions.

3. Results and Discussion

Morphological Characterization of Ferrocene/SWCNT Bundle Hybrid Materials. The mixture of concentrated sulfuric and nitric acids with a volume ratio of 3:1 was chosen here as an effective method for cutting the raw SWCNTs (see Experimental Procedures for details). The pure shortened carbon nanotubes were characterized by AFM, as shown in Figure 1a. The image indicates that the morphology of the SWCNT bundles changed from that of highly entangled strands (data not shown) to flexible rod-like ones that were thoroughly dispersed in ethanol after etching. The length of the shortened carbon nanotube bundles was about 0.5−2 μm. The surface of the nanotubes was smooth. Taking into account AFM tip broadening, some of those apparent individual tubes were actually aggregates of several tubes in van der Waals contact.[16] After ferrocene immobilization, purified ferrocene/SWCNT bundles were dispersed in ethanol and formed a stable suspension, as shown in Figure 1d. SEM analysis indicated that the ferrocene

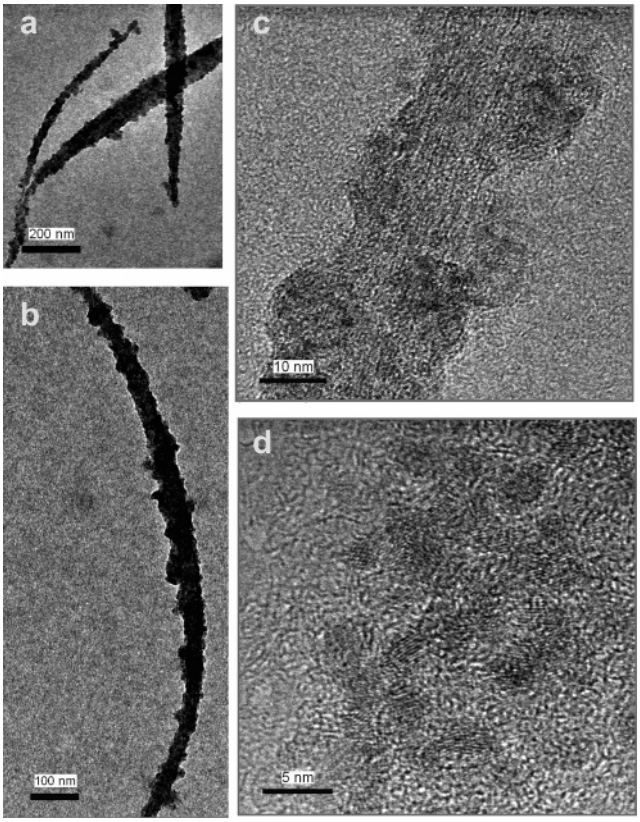

Figure 2. TEM images of a bundle of SWCNT functionalized by ferrocene molecule clusters under different magnifications. The round spots are the (~10 nm) ferrocene molecule clusters on the bundle. Panel d clearly shows the iron cores of ferrocene on the SWCNT bundle.

molecule cluster was densely immobilized on the surface of the SWCNT bundles (Figure 1b). A higher magnification image shows that SWCNT functionalized with ferrocene has a bead string-like structure, indicating the wrapping of ferrocene along SWCNT sidewalls (Figure 1c). The formation is not likely a physical adsorption, as evidenced by the stability of the hybrids when ultrasonicated. We do not observe dissociation of ferrocene from the nanotubes' surface. The mechanism of synthesis of ferrocene/SWCNT may be explained by taking into account the cooperation effect due to the π-stacking between ferrocene and SWCNT and van der Waals interactions between the ferrocene molecules. The ferrocene/SWCNT hybrids are highly stable against desorption in ethanol. We also observe successful immobilization of ferrocene onto SWCNT in the TEM. Figure 2 shows the typical examples of a ferrocene molecule cluster immobilized on a SWCNT bundle under different magnifications. A range of 10 nm ferrocene clusters are clearly resolved. From Figure 2d, the iron cores of each ferrocene are observed as a range of 4 nm, which agrees with the feature reported before.[5a]

To further demonstrate the functionalization of SWCNT with ferrocene, FTIR spectroscopy was conducted. Figure 3 shows the FTIR spectra of pure shortened SWCNT and ferrocoene/SWCNT hybrids. For the ferrocene/SWCNT sample, the peaks at 1652 and 1539 cm^{-1} refer to the IR stretching vibration frequency of carboxylic acid groups (−COOH) and carboxylate groups ($-COO^-$) after oxidation treatment of carbon nanotubes, respectively. The characteristic FTIR peaks of ferrocene are around 3095, 1407, 1107, 1101, and 816 cm^{-1}, which are in agreement with the previous report.[17] This analysis confirms the existence of ferrocene on the SWCNTs in a noncovalent way.

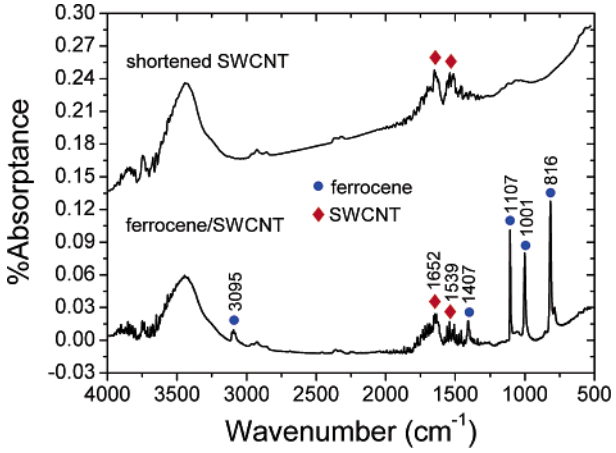

Figure 3. FTIR spectra of pure shortened SWCNT and ferrocene functionalized SWCNT hybrid.

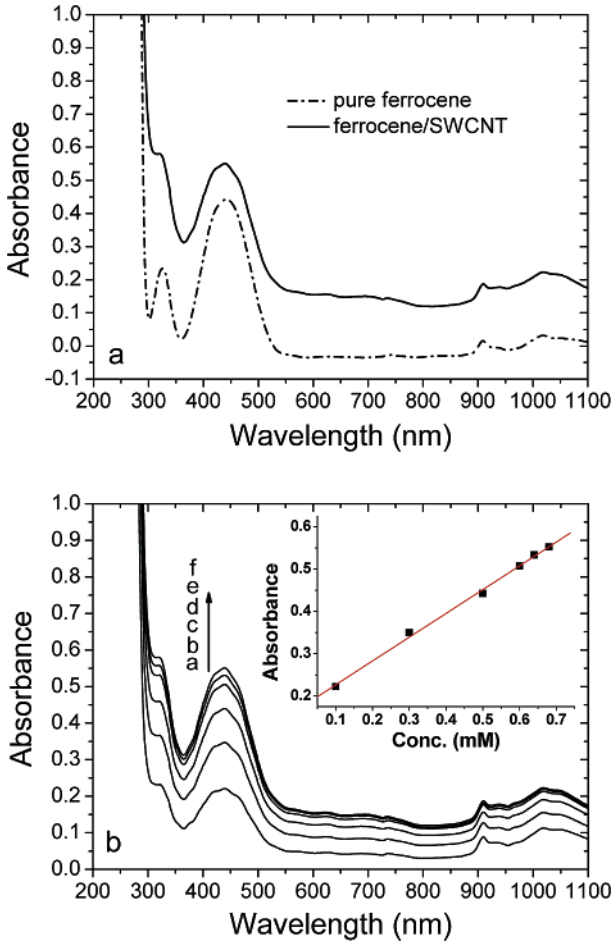

Figure 4. UV−vis spectra of ferrocene founctionalized SWCNT hybrid in ethanol solution. (a) Comparison between pure ferrocene and ferrocene functionalized SWCNT hybrid. (b) UV−vis spectra of ferrocene functionalized SWCNT in a solution of ethanol with volumes of (a) 50, (b) 150, (c) 250, (d) 300, (e) 320, and (f) 340 μL, respectively. The ferrocene/SWCNT hybrid was prepared using 500 μL of 2 mg L^{-1} SWCNT and 50 mL of 0.01 M ferrocene in ethanol. The inset is the relationship of the absorbance with the concentration ($R = 0.998$, the black points are experimental data, and the line is a linear fit through this data; the concentration was calculated using the ferrocene solution).

To show the characteristics and stability of ferrocene functionalized SWCNT hybrids, an analysis of the UV−vis absorption spectrum was carried out. Figure 4 displays the UV−vis spectra of the ferrocene/SWCNT hybrid in ethanol. In comparison with the pure ferrocene UV−vis spectrum (ferrocene

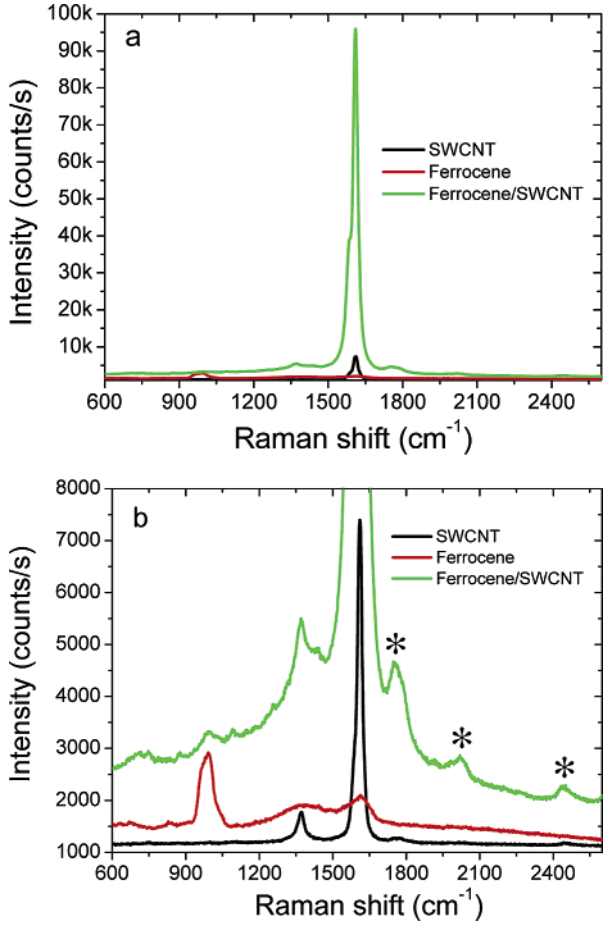

Figure 5. (a) Raman spectra of pure carbon nanotube, ferrocene, and ferrocene functionalized SWCNT. The peaks labeled with asterisks are attributed to the presence of ferrocene. (b) Partial enlarged detail corresponds to panel a. Experimental conditions: 488 nm laser wavelength; 13 mW laser power; 10 s exposure × 10 accumulations.

has absorption peaks in the UV−vis region at 325 nm and at 440 nm in ethanol, Figure 4a), we found that two shoulders at about 415 and 464 nm arose from face-to-face aggregation because of the extensive coupling between the π-electron systems of adjacent rings. Furthermore, the adsorption peak at 325 nm became a shoulder, also indicating that the ferrocene molecules can be immobilized on the surface of the carbon nanotubes. Meanwhile, we obtained the well-regulated UV−vis spectra of different concentrations of ferrocene/SWCNT hybrids in ethanol (Figure 4b). It is necessary to point out first that the hybrid has a high stability in water owing to the water indissolubility of ferrocene. The observed absorbance is linearly dependent on the concentration of the measured sample, indicating that no aggregation of the ferrocene functionalized nanotubes takes place. Besides, it is worth noting that no sediment appeared even though the hybrid/ethanol solution was kept at ambient conditions for more than 3 months.

Raman spectroscopy can provide unique information about vibrational and electronic properties of the material.[18] Thus, it can be used to characterize the structure of the ferrocene/SWCNT hybrid material. Figure 5 shows the Raman spectra for pure carbon nanotubes, pure ferrocene, and ferrocene/SWCNT hybrid. Here, it is seen that, for pure carbon nanotubes, the strong intensity of the G band at about 1612 cm^{-1} corresponds to an in-plane oscillation of carbon atoms in the grapheme sheet. The D Raman band (disorder-induced band) of CNTs, which is observed at about 1370 cm^{-1}, indicates a low level of defects or dangling bonds. Furthermore, the ratio

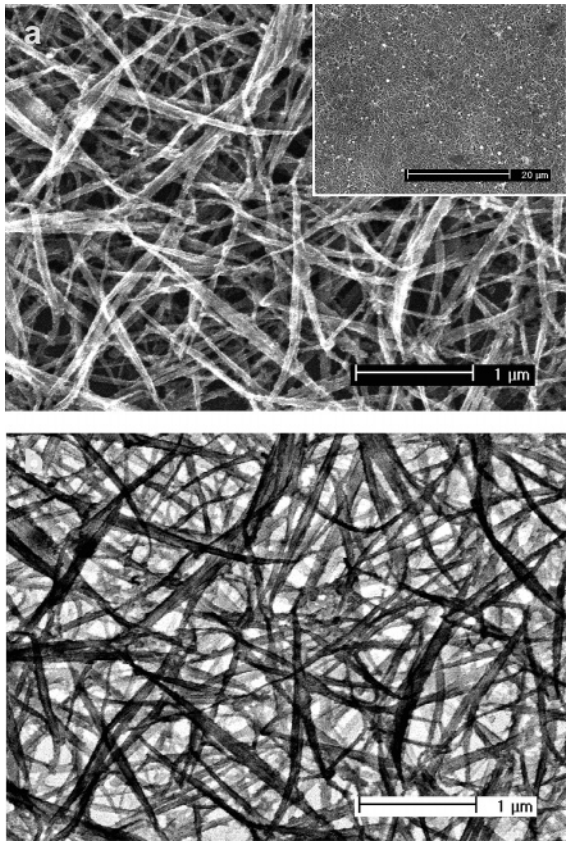

Figure 6. Topography SEM images of the #4 ferrocene/SWCNT electrode. (a) A higher magnification SEM image. The inset shows the lower magnification image of the hybrid film. (b) The photographic negative image corresponds to panel a.

of I_G/I_D is very high, indicating the high quality of single-walled carbon nanotubes.[18b] Here, I_G/I_D refers to the ratio of the intensity of the G and D band features at their most intense points. For the pure ferrocene sample, a narrow peak at about 994 cm^{-1} and two weak broad peaks at bout 1365 and 1612 cm^{-1} can be observed, respectively. However, Raman features for the ferrocene/SWCNT hybrid show a completely different behavior than for pure SWCNT and ferrocene, as seen in Figure 5a. It is worth noting that there is a very strong peak at about 1612 cm^{-1}, indicating that the hybrid material has good metallic features after ferrocene immobilization.[18c] Besides, there are other peaks marked with an asterisk that may be attributed to the presence of ferrocene. The origin of these differences is not clear at present.

Cyclic Voltammogram Behavior of the Ferrocene/SWCNT Electrode. We prepared a set of different ferrocene/SWCNT content electrodes coded as #1, #2, #3, and #4 for biosensing investigations. The detailed preparation procedure of the interdigitated ferrocene/SWCNT electrodes can be obtained from the Experimental Procedures. Briefly, the ferrocene/SWCNT ethanol solution was deposited onto the glass slide and dried, and then a platinum wire was welded onto the ferrocene/SWCNT film with silver paste. After this, the electrode was partly mounted with epoxy resin, and a small area of film was left exposed, which was used to measure the electrochemical properties of the electrode, as well as to detect L-glutamate. Figure 6 depicts the topography SEM images of the ferrocene/SWCNT electrode. We found that the ferrocene/SWCNT hybrid could firmly attach onto a glass substrate and form a uniform film (Figure 6a, inset). This is due to the high dispersity of ferrocene/SWCNT. After dispersion, the SWCNT bundles have a high surface-to-volume ratio and surface free energy, so they

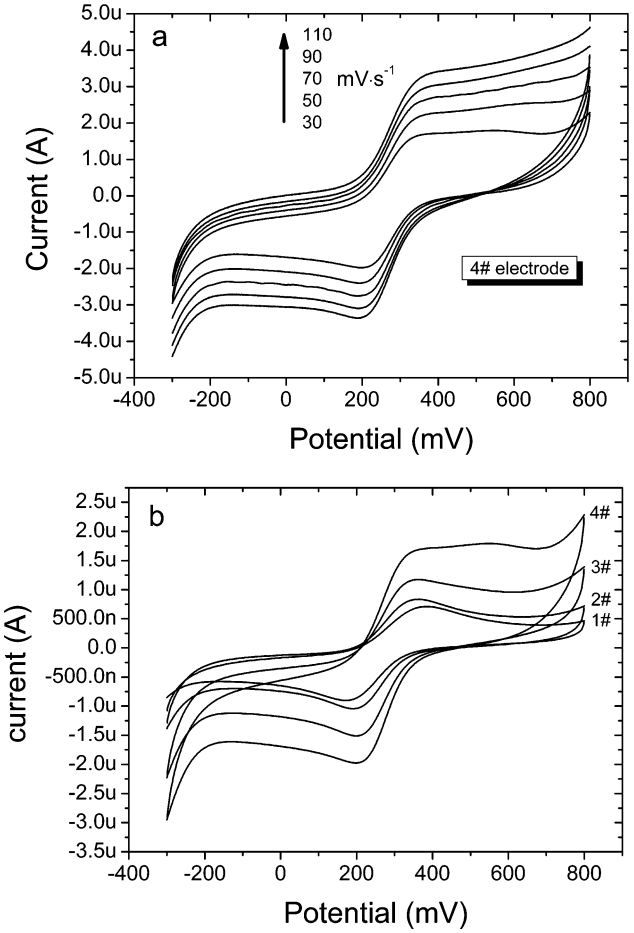

Figure 7. Cyclic voltammograms (CV) of the ferrocene/SWCNT electrode for 0.5 mM $K_3Fe(CN)_6$/PBS solution. (a) CV behavior of #4 electrode at different scan rates (30, 50, 70, 90, and 110 mV s^{-1}). (b) The effect of ferrocene/SWCNT content on CV behavior at a scan rate of 30 mV s^{-1}.

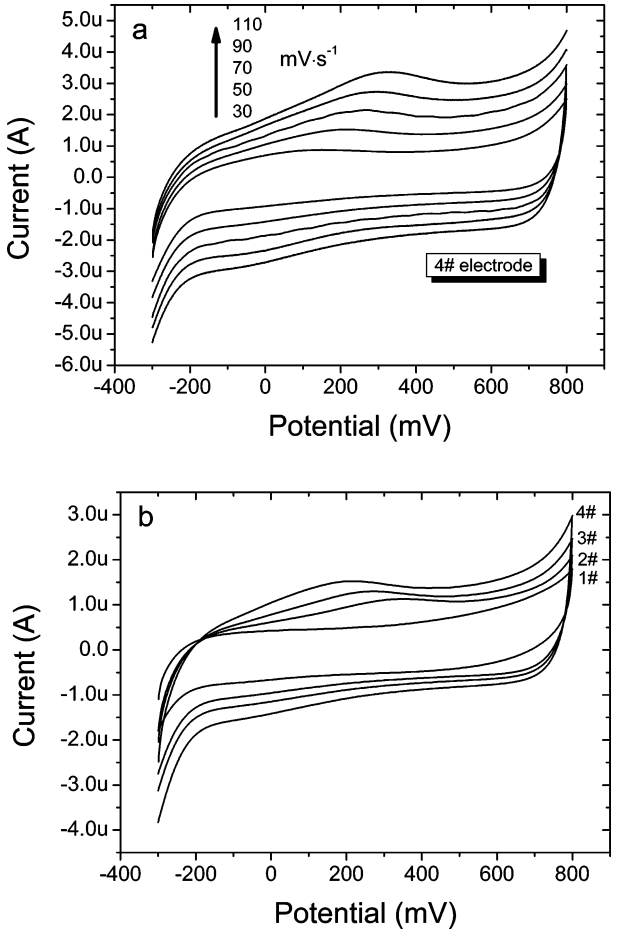

Figure 8. Cyclic voltammograms of ferrocene/SWCNT electrode for 1 μM L-glutamate/PBS solution. (a) CV behavior of the as-studied electrode prepared with given ferrocene/SWCNT content at different scan rates (30, 50, 70, 90, and 110 mV s^{-1}). (b) The effect of ferrocene/SWCNT content on CV behavior at a scan rate of 50 mV s^{-1}.

tend to interact with each other as well as the glass substrate to release some of the free energy while the water evaporates. The strains among any of the nanotubes to form the film are equivalent in all directions since the shortened nanotubes are individually suspended in ethanol. If the nanotubes are not individually suspended in ethanol, the asymmetric strain from the nanotubes will result in an uneven film, which cannot adhere tightly to the glass and will easily peel off when put into solution. A higher magnification image (Figure 6a) and its corresponding photographic negative image (Figure 6b) clearly show that the ferrocene/SWCNT hybrid film has an interdigitated construction. This multilayered construction can be obtained by simply regulating the number of deposition cycles or relative amounts of the ferrocene/SWCNT components within each of the constituent layers. This structure allows the as-studied electrode to have a highly permeable net property; on the other hand, the acid treatment creates more oxide defects on the tube sidewalls and ends, which can be involved in the redox reaction and make the active sites of the ferrocene/SWCNT electrode more hydrophilic so that the sample can contact the surface better.[19]

The redox reactions of potassium ferrocyanide usually serve as a benchmark in investigations of electrochemistry for different electrodes. Here, $Fe(CN)_6^{3-}/Fe(CN)_6^{4-}$ redox pairs were first used to investigate the electrochemical performance of ferrocene/SWCNT electrodes. We found that the catalytic current increased with increasing the ferroncene/SWCNT content in a 0.5 mM $K_3Fe(CN)_6$/PBS solution at scan rate of 30 mV s^{-1}. We also studied the effect of scan rates on electrochemical behavior at the #4 electrode (Figure 7). In the L-glutamate/PBS solution, it was found that the reduction peak potential shifted positively from 115 to 330 mV for different scan rates. Similarly, the catalytic current increased with increasing the ferrocene/SWCNT content at a scan rate of 50 mV s^{-1}. This can be ascribed to the electrocatalytic and kinetic effects of the ferrocene/SWCNT surface on the reduction of l-glutamate (Figure 8).

Real-Time Behavior of the Ferrocene/SWCNT Electrode. The real-time current−concentration behavior of the ferrocene/SWCNT electrode presented in Figure 9a shows that the current increases stepwise with each successive addition of the L-glutamate solution. The response is very fast in reaching to a dynamic equilibrium upon each addition of the sample solution, generating a steady-state current signal within several seconds. This fast response can be explained by the effective transfer of substrate and products through the ferrocene/SWCNT film, resulting from nanosizes of the tube and the unique interdigitated structure of the ferrocene/SWCNT film as described previously. The typical plots of the reduction peak current versus concentration (Figure 9b) show that this concentration dependence is linear over a 1−7 μM range and thus suggests that the ferrocene/SWCNT electrode may function as a nanobiosensor. Since the large slope corresponds to the low detection limit of $K_3Fe(CN)_6$,[15] we suggest that the ferrocene/SWCNT electrodes exhibit better performance in electrochemical responses and that the #4 electrode exhibits the best electrochemical behavior (i.e.,

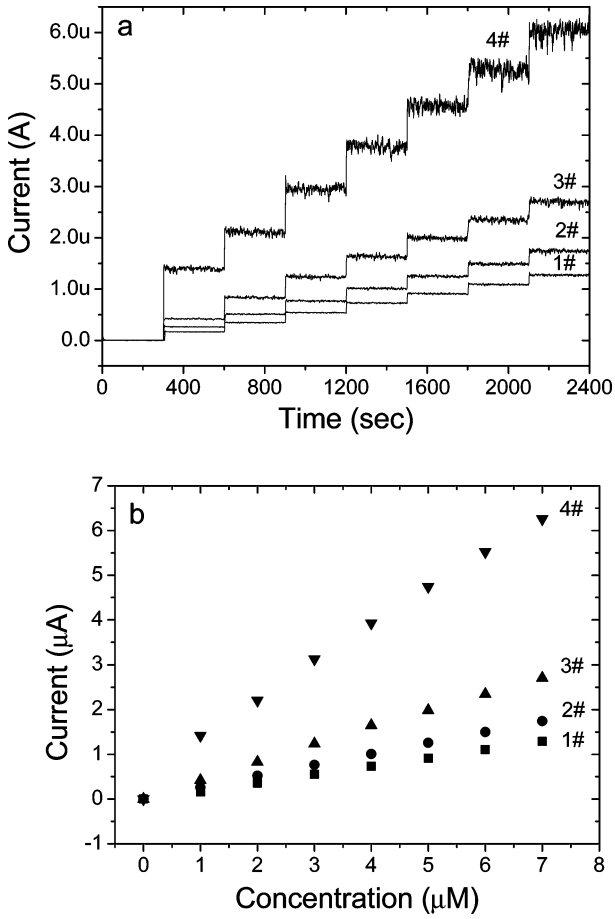

Figure 9. (a) Current responses of L-glutamate biosensor prepared with different ferrocene/SWCNT contents on successive additions of 0.01 M L-glutamate aliquots (1 μL each). The initial potential was 200 mV, sensitivity was 1 μA V^{-1}, and measurement was performed in 10 mL of PBS (pH 7.4) with stirring. (b) Calibration plots the peak current vs concentrations presented in panel a.

the response is dependent on the ferrocene/SWCNT content; higher responses are obtained with higher ferroence/SWCNT contents). At a concentration of 1 μM, for example, the catalytic current is about 4 times larger than that of the #3 electrode and about 10 times larger than that of the #1 electrode. The electron transfer of reactants during electro-oxidation is mainly determined by the conductivity of electrode materials as well as the active functional groups on its surface.[20] For the ferrocene/SWCNT electrode, SWCNT has not only good conductivity but also a much higher surface area, which can accommodate much more ferrocene moclecules in a given region. As we know, ferrocene is a well-known substance as a mediator that can improve the electron transfer of biomolecules with the conductive support in the electrochemical detection. At higher ferrocene/SWCNT contents, more mediators were obtained on the electrode, and consequently, a higher catalytic current was expected.

4. Conclusion

The shortened single-walled carbon nanotubes have been functionalized by ferrocene in a noncovalent way. The ferrocene/SWCNT hybrid has a high stability not only in water but also in an organic solvent such as ethanol and acetone. It demonstrates that no sediment can be observed even though the hybrid/ethanol solution was kept at ambient conditions for more than 3 months. The hybrids can be made into an interdigitated construction film, which firmly attaches onto a glass substrate. With such advantages, we fabricate a set of ferrocene/SWCNT electrodes and use them in the solution phase. Electrochemical experiments indicated that the ferrocene/SWCNT electrode possesses a flat and wide potential window, suggesting that it can be used as an electrode for bioelectrochemical analysis. Owing to the existence of more carbon nanotubes, more active electrochemical mediators, and the unique interdigitated structure of the film, the ferrocene/SWCNT electrode exhibits a high catalytic efficiency, high sensitivity, and fast response during the detection of a low concentration of L-glutamate (1 μM). A good linear relationship between current and concentration was obtained from 1 to 7 μM. We suggest that this study could provide a development in the functionalized carbon nanotube research field. Further studies are being carried out to study the absorptive capacity of ferrocene on carbon nanotubes (i.e., the saturation value), the thickness of the film, and the electrode process kinetics.

Acknowledgment. This work was supported by Brain Korea 21 project, the School of Information Technology, Korea Advanced Institute of Science and Technology in 2006 and the National Research and Development Program (NRDP, 2005-01274) biomedical function monitoring biosensor development sponsored by the Korea Ministry of Science and Technology (MOST).

References and Notes

(1) (a) Kumar, M. K.; Ramaprabhu, S. *J. Phys. Chem. B* **2006**, *110*, 11291−11298. (b) Zhang, Y. M.; Zhang, D. J.; Liu, C. B. *J. Phys. Chem. B* **2006**, *110*, 4671−4674. (c) Bekyarova, E.; Davis, M.; Burch, T.; Itkis, M. E.; Zhao, B.; Sunshine, S.; Haddon, R. C. *J. Phys. Chem. B* **2004**, *108*, 19717−19720. (d) Akola, J.; Rytkönen, K.; Manninen, M. *J. Phys. Chem. B* **2006**, *110*, 5186−5190. (e) Fu, Q.; Liu, J. *J. Phys. Chem. B* **2005**, *109*, 13406−13408. (d) Wang, C. C.; Zhou, G.; Liu, H. T.; Wu, J.; Qiu, Y.; Gu, B. L.; Duan, W. H. *J. Phys. Chem. B* **2006**, *110*, 10266−10271. (g) Katz, E.; Willner, I. *ChemPhysChem* **2004**, *5*, 1084−1104.

(2) (a) Davis, J. J.; Coleman, K. S.; Azamian, B. R.; Bagshaw, C. B.; Green, M. L. H. *Chem.—Eur. J.* **2003**, *9*, 3732−3739. (b) Ionescu, R.; Espinosa, E. H.; Sotter, E.; Llobet, E.; Vilanova, X.; Correig, X.; Felten, A.; Bittencourt, C.; Van Lier, G.; Charlier, J. C.; Pireaux, J. J. *Sens. Actuators, B* **2006**, *113*, 36−46. (c) Su, P. G.; Sun, Y. L.; Lin, C. C. *Sens. Actuators, B* **2006**, *115*, 338−343. (d) Huang, X. J.; Li, Y.; Im, H. S.; Yarimaga, O.; Kim, J. H.; Jang, D. Y.; Cho, S. O.; Cai, W. P.; Choi, Y. K. *Nanotechnology* **2006**, *17*, 2988−2993. (e) Huang, X. J.; Im, H. S.; Yarimaga, O.; Kim, J. H.; Jang, D. Y.; Lee, D. H.; Kim, H. S.; Choi, Y. K. *J. Electroanal. Chem.* **2006**, 594, 27−34. (f) Wang, J.; Musameh, M. *Anal. Chem.* **2003**, *75*, 2075−2079. (g) Wang, J.; Hocevar, S. B.; Ogorevc, B. *Electrochem. Commun.* **2004**, *6*, 176−179. (h) Patolsky, F.; Weizmann, Y.; Willner, I. *Angew. Chem.* **2004**, *116*, 2165−2169 and Ibid, *Angew. Chem., Int. Ed.* **2004**, *43*, 2113−2117.

(3) (a) Diao, P.; Liu, Z. F. *J. Phys. Chem. B* **2005**, *109*, 20906−20913. (b) Diao, P.; Liu, Z. F.; Wu, B.; Nan, X. L.; Zhang, J.; Wei, Z. *ChemPhysChem* **2002**, *3*, 898−901. (c) Liu, Z. F.; Shen, Z. Y.; Zhu, T.; Hou, S. F.; Ying, L. Z.; Shi, Z. J.; Gu, Z. N. *Langmuir* **2000**, *16*, 3569−3573. (d) Gooding, J. J.; Wibowo, R.; Liu, J.; Yang, W.; Losic, D.; Orbons, S.; Mearns, F. J.; Shapter, J. G.; Hibbert, D. B. *J. Am. Chem. Soc.* **2003**, *125*, 9006−9007.

(4) (a) Jiang, K. Y.; Schadler, L. S.; Siegel, R. W.; Zhang, X. J.; Zhang, H. F.; Terrones, M. *J. Mater. Chem.* **2004**, *14*, 37−39. (b) Moghaddam, M. J.; Taylor, S.; Gao, M.; Huang, S.; Dai, L. M.; McCall, M. J. H. *Nano Lett.* **2004**, *4*, 89−93. (c) Hazani, M.; Naaman, R.; Hennrich, F.; Kappes, M. M. *Nano Lett.* **2003**, *3*, 153−155. (d) Peng, H. Q.; Alemany, L. B.; Margrave, J. L.; Khabasheku, V. N. *J. Am. Chem. Soc.* **2003**, *125*, 15174−15182.

(5) (a) Chen, R. J.; Zhang, Y. G.; Wang, D. W.; Dai, H. J. *J. Am. Chem. Soc.* **2001**, *123*, 3838−3839. (b) Satake, A.; Miyajima, Y.; Kobuke, Y. *Chem. Mater.* **2005**, *17*, 716−724. (c) Murakami, H.; Nomura, T.; Nakashima, N. *Chem. Phys. Lett.* **2003**, *378*, 481−485. (d) Katz, E. *J. EIectroanal. Chem.* **1994**, *365*, 157−164. (e) Jaegfeldt, H.; Kuwana, T.; Johanssont, G. *J. Am. Chem. Soc.* **1983**, *105*, 1805−1814.

(6) (a) Liu, J. Y.; Tian, S. J.; Tiefenauer, L.; Nielsen, P. E.; Knoll, W. *Anal. Chem.* **2005**, *77*, 2756−2761. (b) Flechsig, G. U.; Peter, J.; Hartwich, G.; Wang, J.; Grundler, P. *Langmuir* **2005**, *21*, 7848−7853. (c) He, P. G.; Dai, L. M. *Chem. Commun.* **2004**, *6*, 348−349. (d) Yabuki, S.; Mizutani, F.; Hirata, Y. *Sens. Actuators, B* **2000**, *65*, 49−51.

(7) Guldi, D. M.; Marcaccio, M.; Paolucci, D.; Paolucci, F.; Tagmatarchis, N.; Tasis, D.; Vázquez, E.; Prato, M. *Angew. Chem., Int. Ed.* **2003**, *42*, 4206−4209.

(8) (a) Callegari, A.; Marcaccio, M.; Paolucci, D.; Paolucci, F.; Tagmatarchis, N.; Tasis, D.; Vázquez, E.; Prato, M. *Chem. Commun.* **2003**, 2576−2577. (b) Callegari, A.; Cosnier, S.; Marcaccio, M.; Paolucci, D.; Paolucci, F.; Georgakilas, V.; Tagmatarchis, N.; Vázquez, E.; Prato, M. *J. Mater. Chem.* **2004**, *14*, 807−810. (c) Kandimalla, V. B.; Tripathi, V. S.; Ju, H. X. *Biomaterials* **2006**, *27*, 1167−1174.

(9) Yang, X. Y.; Lu, Y. H.; Ma, Y. F.; Li, Y. J.; Du, F.; Chen, Y. S. *Chem. Phys. Lett.* **2006**, *420*, 416−420.

(10) (a) Hafkenscheid, J. C. M.; Dijt, C. C. M. *Clin. Chem.* **1979**, *25*, 55−59. b) Sampson, E. J.; Whitner, V. S.; Burtis, C. A.; McKneaily, S. S.; Fast, D. M.; Bayse, D. D. *Clin. Chem.* **1980**, *26*, 1156−1164. (c) Purcell, G. V.; Behenna, D. B.; Walsh, P. R. *Clin. Chem.* **1979**, *25*, 780−782.

(11) Zhang, M.; Mullens, C.; Gorski, W. *Electrochim. Acta* **2005**, *51*, 4528−4532 and Ibid, *Electroanalysis* **2005**, *17*, 2114−2120.

(12) (a) Yao, T.; Nanjyo, Y.; Tanaka, T.; Nishino, H. *Electroanalysis* **2001**, *13*, 1361−1366. (b) Hayashi, K.; Kurita, R.; Horiuchi, T.; Niwa, O. *Biosens. Bioelectron.* **2003**, *18*, 1249−1255. (c) Rahman, M. A.; Kwon, N. H.; Won, M. S.; Choe, E. S.; Shim, Y. S. *Anal. Chem.* **2005**, *77*, 4854−4860. (d) McMahon, C. P.; O'Neill, R. D. *Anal. Chem.* **2005**, *77*, 1196−1199. (e) McMahon, C. P.; Rocchitta, G.; Serra, P. A.; Kirwan, S. M.; Lowry, J. P.; O'Neill, R. D. *Anal. Chem.* **2006**, *78*, 2352−2359.

(13) Hasebe, Y.; Gu, T. T.; Kusakabe, H. *Electrochemistry* **2006**, *74*, 179−182.

(14) You, T. Y.; Niwa, O.; Kurita, R.; Iwasaki, Y.; Hayashi, K.; Suzuki, K.; Hirono, S. *Electroanalysis* **2004**, *16*, 54−59.

(15) Boo, H.; Jeong, R. A.; Park, S.; Kim, K. S.; An, K. H.; Lee, Y. H.; Han, J. H.; Kim, H. C.; Chung, T. D. *Anal. Chem.* **2006**, *78*, 617−620.

(16) Liu, J.; Rinzler, A. G.; Dai, H. J.; Hafner, J. H.; Bradley, R. K.; Boul, P. J.; Lu, A.; Iverson, T.; Shelimov, K.; Huffman, C. B.; Rodriguez-Macias, F.; Shon, Y. S.; Lee, T. R.; Colbert, D. T.; Smalley, R. E. *Science* **1998**, *280*, 1253−1256.

(17) Guan, L. H.; Shi, Z. J.; Li, M. X.; Gu, Z. N. *Carbon* **2005**, *43*, 2780−2785.

(18) (a) Zhao, Q.; Wagner, H. D. *Philos. Trans. R. Soc. London, Ser. A* **2004**, *362*, 2407−2424. (b) Lu, J. Q.; Moll, N.; Fu, Q.; Liu, J. *Chem. Mater.* **2005**, *17*, 2237−2240. (c) Brown, S. D. M.; Jorio, A.; Dresselhaus, M. S.; Dresselhaus, G. *Phys. Rev. B* **2001**, *64*, 073403−073406

(19) (a) Banks, C. E.; Davies, T. J.; Wildgoose, G. G.; Compton, R. G. *Chem. Commun.* **2005**, *7*, 829−841. (b) Banks, C. E.; Moore, R. R.; Davies, T. J.; Compton, R. G. *Chem. Commun.* **2004**, *16*, 1804−1805. (c) Chou, A.; Böcking, T.; Singh, N. K.; Gooding, J. J. *Chem. Commun.* **2005**, *7*, 842−844.

(20) Hu, C. G.; Zhang, Y. Y.; Bao, G.; Zhang, Y. L.; Liu, M. L.; Wang, Z. L. *Chem. Phys. Lett.* **2005**, *418*, 520−525 and Ibid, *J. Phys. Chem. B* **2005**, *109*, 20072−20076.